Localization-based super-resolution microscopy with an sCMOS camera

Zhen-Li Huang,[1,2,4,5] Hongyu Zhu,[1,2,4] Fan Long,[1,2,4] Hongqiang Ma,[1,2] Lingsong Qin,[1,2] Yongfeng Liu,[3] Jiuping Ding,[3] Zhihong Zhang,[1,2] Qingming Luo,[1,2] and Shaoqun Zeng[1,2,5]

[1] *Britton Chance Center for Biomedical Photonics, Wuhan National Laboratory for Optoelectronics-Huazhong University of Science and Technology, Wuhan 430074, China*
[2] *Key Laboratory of Biomedical Photonics of Ministry of Education, Huazhong University of Science and Technology, Wuhan 430074, China*
[3] *Key Laboratory of Molecular Biophysics of Ministry of Education, College of Life Science and Technology, Huazhong University of Science and Technology, Wuhan 430074, China*
[4] *These authors contributed equally to this work.*
[5] *sqzeng@mail.hust.edu.cn*
[5] *leo@mail.hust.edu.cn*

Abstract: In the community of localization-based super-resolution microscopy (or called localization microscopy), it is generally believed that the emission of single molecules is so weak that an EMCCD (electron multiplying charge coupled device) camera is necessary to be used as the detector by eliminating read noise. Here we evaluate the possibility of a new kind of low light detector, scientific complementary metal-oxide-semiconductor (sCMOS) camera in localization microscopy. We demonstrate experimentally that sCMOS is capable of imaging actin bundles with FWHM diameter of 37 nm, evidencing the capability of sCMOS in localization microscopy. We further characterize the noise performance of sCMOS and find out that, with the use of a bright fluorescence probe such as d2EosFP, localization microscopy imaging is now working in the shot noise limited region.

OCIS codes: (180.2520) Fluorescence microscopy; (100.6640) Superresolution; (040.3780) Low light level.

References and links

1. X. Michalet, O. H. W. Siegmund, J. V. Vallerga, P. Jelinsky, J. E. Millaud, and S. Weiss, "Detectors for single-molecule fluorescence imaging and spectroscopy," J. Mod. Opt. **54**(2-3), 239–281 (2007).
2. W. E. Moerner and D. P. Fromm, "Methods of single-molecule fluorescence spectroscopy and microscopy," Rev. Sci. Instrum. **74**(8), 3597–3619 (2003).
3. E. Betzig, G. H. Patterson, R. Sougrat, O. W. Lindwasser, S. Olenych, J. S. Bonifacino, M. W. Davidson, J. Lippincott-Schwartz, and H. F. Hess, "Imaging intracellular fluorescent proteins at nanometer resolution," Science **313**(5793), 1642–1645 (2006).
4. S. T. Hess, T. P. K. Girirajan, and M. D. Mason, "Ultra-high resolution imaging by fluorescence photoactivation localization microscopy," Biophys. J. **91**(11), 4258–4272 (2006).
5. M. J. Rust, M. Bates, and X. W. Zhuang, "Sub-diffraction-limit imaging by stochastic optical reconstruction microscopy (STORM)," Nat. Methods **3**(10), 793–796 (2006).
6. B. Huang, M. Bates, and X. W. Zhuang, "Super-resolution fluorescence microscopy," Annu. Rev. Biochem. **78**(1), 993–1016 (2009).
7. M. Fernández-Suárez and A. Y. Ting, "Fluorescent probes for super-resolution imaging in living cells," Nat. Rev. Mol. Cell Biol. **9**(12), 929–943 (2008).
8. M. Bigas, E. Cabruja, J. Forest, and J. Salvi, "Review of CMOS image sensors," Microelectron. J. **37**(5), 433–451 (2006).
9. B. Fowler, C. A. Liu, S. Mims, J. Balicki, W. Li, H. Do, J. Appelbaum, and P. Vu, "A 5.5Mpixel 100 frames/sec wide dynamic range low noise CMOS image sensor for scientific applications," Proc. SPIE **7536**, 753607, 753607-12 (2010).
10. S. A. Jones, S. H. Shim, J. He, and X. Zhuang, "Fast, three-dimensional super-resolution imaging of live cells," Nat. Methods **8**(6), 499–505 (2011).

#151443 - $15.00 USD Received 22 Jul 2011; revised 31 Aug 2011; accepted 5 Sep 2011; published 19 Sep 2011

11. T. W. Quan, S. Q. Zeng, and Z. L. Huang, "Localization capability and limitation of electron-multiplying charge-coupled, scientific complementary metal-oxide semiconductor, and charge-coupled devices for superresolution imaging," J. Biomed. Opt. **15**(6), 066005 (2010).
12. K. I. Mortensen, L. S. Churchman, J. A. Spudich, and H. Flyvbjerg, "Optimized localization analysis for single-molecule tracking and super-resolution microscopy," Nat. Methods **7**(5), 377–381 (2010).
13. J. R. Janesick, *Photon transfer: DN [lambda]* (SPIE, Bellingham, Wash., 2007), pp. xiv, 258 p.
14. P. N. Hedde, J. Fuchs, F. Oswald, J. Wiedenmann, and G. U. Nienhaus, "Online image analysis software for photoactivation localization microscopy," Nat. Methods **6**(10), 689–690 (2009).
15. J. Lippincott-Schwartz and G. H. Patterson, "Photoactivatable fluorescent proteins for diffraction-limited and super-resolution imaging," Trends Cell Biol. **19**(11), 555–565 (2009).
16. K. Nienhaus, G. U. Nienhaus, J. Wiedenmann, and H. Nar, "Structural basis for photo-induced protein cleavage and green-to-red conversion of fluorescent protein EosFP," Proc. Natl. Acad. Sci. U.S.A. **102**(26), 9156–9159 (2005).
17. J. Wiedenmann and G. U. Nienhaus, "Live-cell imaging with EosFP and other photoactivatable marker proteins of the GFP family," Expert Rev. Proteomics **3**(3), 361–374 (2006).
18. M. S. Robbins and B. J. Hadwen, "The noise performance of electron multiplying charge-coupled devices," IEEE Trans. Electron. Dev. **50**(5), 1227–1232 (2003).
19. T. W. Quan, H. Y. Zhu, X. M. Liu, Y. F. Liu, J. P. Ding, S. Q. Zeng, and Z. L. Huang, "High-density localization of active molecules using Structured Sparse Model and Bayesian Information Criterion," Opt. Express **19**(18), 16963–16974 (2011).
20. R. Yuste and A. Konnerth, *Imaging in neuroscience and development: a laboratory manual* (Cold Spring Harbor Laboratory Press, Cold Spring Harbor, N.Y., 2005).

1. Introduction

Low-light detectors are essential for fluorescence imaging of single molecules [1,2], and thus in realizing several innovative localization-based super-solution imaging techniques, such as photoactivated localization microscopy (PALM) [3,4] and stochastic optical reconstruction microscopy (STORM) [5]. These techniques, which are recently called single molecule localization microscopy or localization microscopy (LM), rely on detection and localization of single fluorescent molecules to reconstruct a super-resolution image with unprecedented spatial resolution, which is not limited by the diffraction of light but by photon statistics [6]. Currently, the typical detector for LM is EMCCD, which eliminates camera read noise and thus could detect extremely weak fluorescence signal. On the other hand, in recent years a significant effort in the super-resolution microscopy community has been focused in the development of brighter fluorescence probes [7], which in principle could provide new possibility for other low-light detectors to be used in LM and thus will surely enable the super-solution imaging techniques to have a widespread impact in diverse applications.

Driven by the imaging demands of high-volume consumer applications such as cell phone cameras and video cameras, in the past several years great improvements have been make to the sensor design and fabrication in the complementary metal oxide semiconductor (CMOS) technology [8], and a new generation of CMOS camera, called sCMOS, has become available in the market, which offers simultaneously extremely low noise, rapid frame rates and large field of view [9]. Since its launch in late 2010, sCMOS has been intensively discussed to have potential capability to become a technology replacement for EMCCD. However, it is not clear whether the relatively high read noise and low photon sensitivity would be two major obstructions for such replacement. Here we report a quantitative evaluation and comparison on the single molecule imaging performance of a Hamamatsu ORCA-Flash2.8 sCMOS and a popular back-illuminated Andor iXon 897 EMCCD. To the authors' knowledge, this is the first experimental report verifying the applicability of sCMOS in LM.

2. Experimental

2.1 Cell culture and plasmid transfection

HEK293T cells were maintained in a humidified incubator at 37 °C with 5% CO_2 and grown in Dulbecco's modified Eagle's medium (DMEM, Invitrogen) containing 10% fetal bovine serum (FBS), 100 U/ml penicillin, and 100mg/ml streptomycin. The day before transfection, cells were seeded on 25-mm-diameter No. 1.5 cover-glass-bottom dishes (Electron Microscopy Sciences, Cat. # 72225-01) grown to 80% confluence. The eukaryotic expression vector for actin bundles labelling, pcDNA3-lifeact-d2EosFP, is a generous gift from Prof.

#151443 - $15.00 USD Received 22 Jul 2011; revised 31 Aug 2011; accepted 5 Sep 2011; published 19 Sep 2011

Gerd Ulrich Nienhaus. Transfection was carried out using Lipofectamine 2000 (Invitrogen) according to the manufacturer's instructions. After that, cells were maintained for 24 h in culture medium and then fixed for imaging.

2.2 Optical setup for localization microscopy

The optical setup for LM imaging was based on an Olympus IX 71 inverted optical microscope and is shown in Fig. 1. Samples were photoconverted from a green fluorescent form to a red fluorescent form with a 405 nm laser diode and excited with a 561 nm diode-pumped solid-state laser (both from CNILaser, China). Neutral density (ND) filters were used to control the laser intensity, and two electronic shutters (UNIBLITZ VS14, Vincent Associates) were used to control the duration of laser irradiance. The laser beams were combined with aluminium mirrors M1-M3 and a dichroic mirror DM1, expanded by a telescope consisting of lenses L1 (focal length = 38.1 mm) and L2 (focal length = 200 mm), spatially filtered with an iris and focused into the back focal plane of a 100x/NA1.49 oil immersion TIRF objective (UAPON 100XOTIRF, Olympus) or a 60x/NA1.42 oil immersion objective (PLAPON 60XO, Olympus) by lens L3 (focal length = 250 mm). The fluorescence was collected with the same objective, passed through a dichroic mirror DM2 (Di01-R488/561, Semrock), filtered with a longpass filter (BLP01-561R-25, Semrock), directed by a movable 100% reflection light-path prism (M5) and focused either onto an Andor iXon 897 EMCCD camera with a standard Olympus 1X C-mount adapter (TL1), or a Hamamatsu ORCA-Flash2.8 sCMOS camera with a standard Olympus tube lens (TL2, focal length = 180 mm), a 100% reflection light-path prism (M6) and a 0.5X C-mount adapter. Data were acquired by the software provided by the camera manufacturers. The image analysis was from an Image J plugins written in Java by our group. Sample drift was checked to be negligible using the method based on correlation function analysis [10], thus was not corrected.

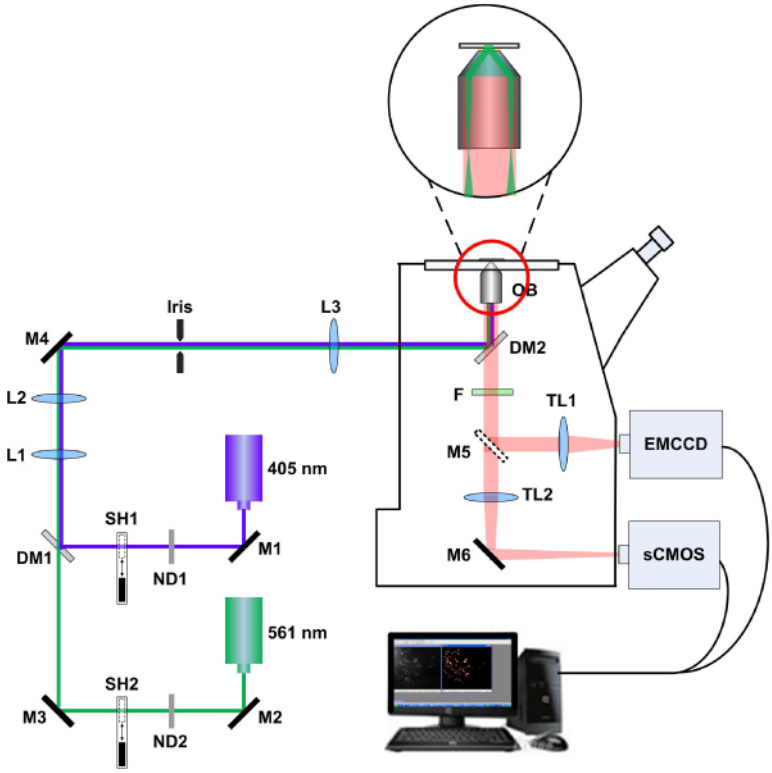

Fig. 1. Optical setup for localization microscopy imaging.

#151443 - $15.00 USD Received 22 Jul 2011; revised 31 Aug 2011; accepted 5 Sep 2011; published 19 Sep 2011

2.2 Data analysis for localization microscopy

In a previous paper, we established a theoretical model to quantify the performance of sCMOS and EMCCD in localization microscopy [11]. Briefly, Gaussian fitting with the following equation was used to localize the single molecules in conventional fluorescence microscopy images.

$$I = I_{sig} \times \exp(-\frac{(i-x_0)^2 + (j-y_0)^2}{2s^2}) + I_{bkg}$$

Here (x0, y0) is the position of fluorescent molecule, s is the width of Gaussian kernel, and I_{sig} and I_{bkg} denote the peak value of signal and the intensity of background photon (including background fluorescence, remnant laser scattering and average readout noise), respectively.

The localization precision for individual fluorescent molecule imaged by sCMOS camera could be calculated by:

$$< \Delta x^2 >= \frac{s^2 + a^2/12}{\phi N} + \frac{8\pi s^4 (\phi I_b + N_r{}^2)}{a^2 (\phi N)^2}$$

For EMCCD camera, the above equation should be modified to:

$$< \Delta x^2 >= \frac{2s^2 + a^2/12}{\phi N} + \frac{8\pi s^4 (\phi I_b)}{a^2 (\phi N)^2}$$

where *s* is the width of Gaussian kernel, *a* is the pixel size, I_b is the background photon ($I_b = I_{bkg}\text{-}N_r^2$), N_r is the readout noise, ϕ is the quantum efficiency and *N* is the number of the photons collected. Note that the above equation was verified by simulation data, although it is slightly different from literature [12].

The signal-noise-ratio (SNR) and signal-background-ratio (SBR) can be calculated from an experimental image by:

$$SNR = \frac{I_{sig}}{\sqrt{I_{sig} + \sigma^2_{I_{bkg}}}}$$

$$SBR = \frac{I_{sig}}{I_{bkg}}$$

Here σ denotes the standard deviation of the background photon, which could be calculated from the surrounding pixels next to the single molecule point spread function (Airy disk).

2.3 Optical setup for photon transfer curve measurements

The optical setup for photon transfer curve (PTC) measurements is shown in Fig. 2. A tungsten-halogen light source (HL-2000-FHSA-LL, Ocean Optics, USA) was guided by a fiber (P1000-2-UV-Vis, Ocean Optics, USA), collimated by a glass lens (focal length = 10 mm) and another glass lens (focal length = 30 mm), modulated by a bandpass filter (FF01-580/14-25, Semrock, USA), attenuated by neutral filters, and then focused into an integrating sphere (Φ170 mm) by a glass lens (focal length = 30 mm). The output light from the integrating sphere, which was found to have a peak wavelength at 580 nm and FWHM of 25 nm, was used for further PTC measurements. All the exposure time was set to be 50 ms unless specified otherwise. The illumination uniformity was defined as the standard deviation divided by the mean, multiplied by 100 percent [13]. In our experiments, a relatively uniform region (80 x 80 pixels for sCMOS, and 50 x 50 pixels or 70 x 70 pixels for EMCCD) in the center of the images was chosen for PTC analysis. In this region, the illumination uniformity was calculated to be better than 99.5%. The PTC measurements were repeated three times.

#151443 - $15.00 USD Received 22 Jul 2011; revised 31 Aug 2011; accepted 5 Sep 2011; published 19 Sep 2011

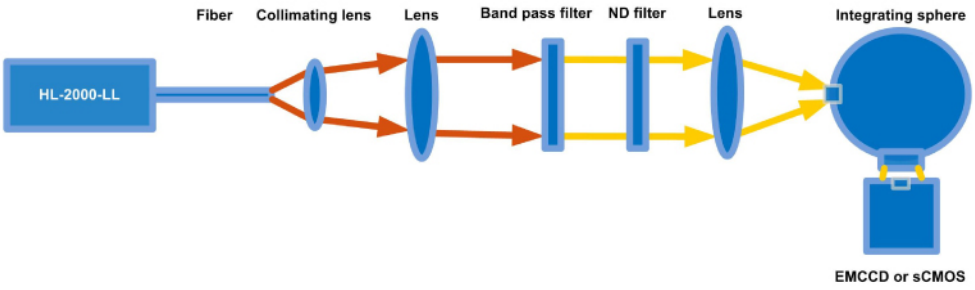

Fig. 2. The optical setup for photon transfer curve (PTC) measurements

2.4 Data analysis for photon transfer curve measurements

2.4.1 Measuring spatial read noise

Set detector parameters (such as gain, exposure time and binning, et al), close the light source shutter block stray light from entering the detectors, and then acquire 100 image frames continuously. Then the spatial read noise can be calculated according to the following equations [13]:

$$\sigma^2_{\mathrm{Re}ad,DN} = \sigma^2_{DifferencedFrames,DN} = \frac{\sum_{j=1}^{99}\sum_{i=1}^{Np}\{[S(j)_i - M(j)] - [S(j+1)_i - M(j+1)]\}^2}{2\times 99\times Np} \quad (1)$$

$$Spatial\ \ read\ \ noise = \sigma_{\mathrm{Re}ad,DN}$$

For sCMOS,

$$OFF_i = \frac{\sum_{j=1}^{100} X(j)_i}{100}$$

$$M(j) = \frac{\sum_{i=1}^{Np}[X(j)_i - OFF_i]}{Np}$$

$$S(j)_i = X(j)_i - OFF_i$$

For EMCCD,

$$OFF = \frac{\sum_{j=1}^{100}\sum_{i=1}^{Np} X(j)_i}{100\times Np}$$

$$M(j) = \frac{\sum_{i=1}^{Np} X(j)_i}{Np} - OFF$$

$$S(j)_i = X(j)_i - OFF$$

Here, $X(j)_i$ is the i_{th} pixel raw value in the j_{th} frame. $S(j)_i$ is the i_{th} pixel signal value in the j_{th} frame after the offset value is removed. OFF_i and OFF are the i_{th} pixel average offset for sCMOS and the average offset for the EMCCD of the 100 dark frames respectively. M(j) is the average of all pixel values in the j_{th} frame after the offset value is removed. Np is the number of pixels in analysis.

#151443 - $15.00 USD Received 22 Jul 2011; revised 31 Aug 2011; accepted 5 Sep 2011; published 19 Sep 2011

2.4.2 Measuring the temporal read noise of sCMOS

Set detector parameters (such as gain, exposure time and binning, et al), close the light source shutter block stray light from entering the detectors, and then acquire 100 image frames continuously. Then the temporal read noise of an individual pixel in sCMOS could be calculated with the following equations [13]:

$$\sigma(i)^2_{\mathrm{Re}ad,DN,temporal} = \frac{\sum_{j=1}^{100}[X(j)_i - M_i]^2}{100} \tag{2}$$

$$Temporal\ \ read\ \ noise = \sigma_{\mathrm{Re}ad,DN,temporal}$$

Here $X(j)_i$ is the i_{th} pixel raw values in the j_{th} frame. M_i is the mean value of the i_{th} pixel of the 100 frames.

2.4.3 Measuring total noise, shot noise and fixed pattern noise

Set gain and binning, open the light source shutter, adjust the ND filters to obtain an appropriate input power, and then acquire 100 image frames continuously. Repeat the measurement with increased input power until the detector was saturated. Then the total noise, shot noise and fixed pattern noise can be obtained with the following equations [13]:

$$\sigma^2_{Total,DN} = \frac{\sum_{j=1}^{100}\sum_{i=1}^{Np}[S(j)_i - M(j)]^2}{100\times Np} \tag{3}$$

$$\sigma^2_{Shot,DN} + \sigma^2_{\mathrm{Re}ad,DN} = \sigma^2_{DifferencedFrames,DN}$$
$$= \frac{\sum_{j=1}^{99}\sum_{i=1}^{Np}\{[S(j)_i - M(j)] - [S(j+1)_i - M(j+1)]\}^2}{2\times 99\times Np} \tag{4}$$

$$\sigma^2_{Shot,DN} = \sigma^2_{DifferencedFrames,DN} - \sigma^2_{\mathrm{Re}ad,DN} \tag{5}$$

$$\sigma^2_{FP,DN} = \sigma^2_{Total,DN} - \sigma^2_{\mathrm{Re}ad,DN} - \sigma^2_{Shot,DN} \tag{6}$$

$$Signal_{DN} = \frac{\sum_{j=1}^{100}\sum_{i=1}^{Np}S(j)_i}{100\times Np} \tag{7}$$

For sCMOS,

$$K_{ADC}(e/DN) = \frac{Signal_{DN}}{\sigma^2_{Shot,DN}} \tag{8}$$

Here, $Signal_{DN}$ is the average signal after the offset value is removed. K_{ADC}(e/DN) is the camera conversion factor (converting the digital number to electron). Then,

$$Total\ \ noise = \sigma_{Total,DN}$$

$$Shot\ \ noise = \sigma_{Shot,DN}$$

$$FP\ \ noise = \sigma_{FP,DN}$$

#151443 - $15.00 USD Received 22 Jul 2011; revised 31 Aug 2011; accepted 5 Sep 2011; published 19 Sep 2011

3. Results and discussion

3.1 The applicability of sCMOS in LM

We evaluated low light imaging performance of the Flash2.8 sCMOS by taking single molecule images (Fig. 3) with a home-built optical setup (Fig. 1), which consists typical components for PALM [3, 6]. To reduce background fluorescence, a total internal reflection fluorescence geometry was used to image actin bundles in fixed HEK293T cells, which was labelled by transient transfection the cells with a plasmid encoding a fusion construct of the actin-binding peptide Lifeact with d2EosFP [14]. The green-to-red photoconvertible fluorescent proteins, d2EosFP, is one of the green-to-red highlighters in the EosFP family with excellent overall performance for LM [15]. Under weak 405 nm light illumination, d2EosFP undergoes a green-to-red photoconvertion and could emit red fluorescence under 561 nm light excitation [16, 17].

After single molecule detection and localization from a stack of 2000 TIRF image frames captured with the Flash2.8 sCMOS (Fig. 3a), notable resolution improvement is visualized in the morphology of actin cytoskeleton structure (Fig. 3b), which is consistent with the result taken with the iXon 897 EMCCD (Fig. 3d). Quantitative analysis on the LM images show that the mean number of total collected photons from d2EosFP is 828 for the Flash2.8 sCMOS (Fig. 3e), which is only ~12% lower than that by the iXon 897 EMCCD (Fig. 3h) and is consistent with the value reported in the literature [10]. With a mean SNR of 5.2 (Fig. 3f) and a localization precision (measured in standard deviation) of 18 nm (Fig. 3g), the applicability of sCMOS in LM is clearly confirmed.

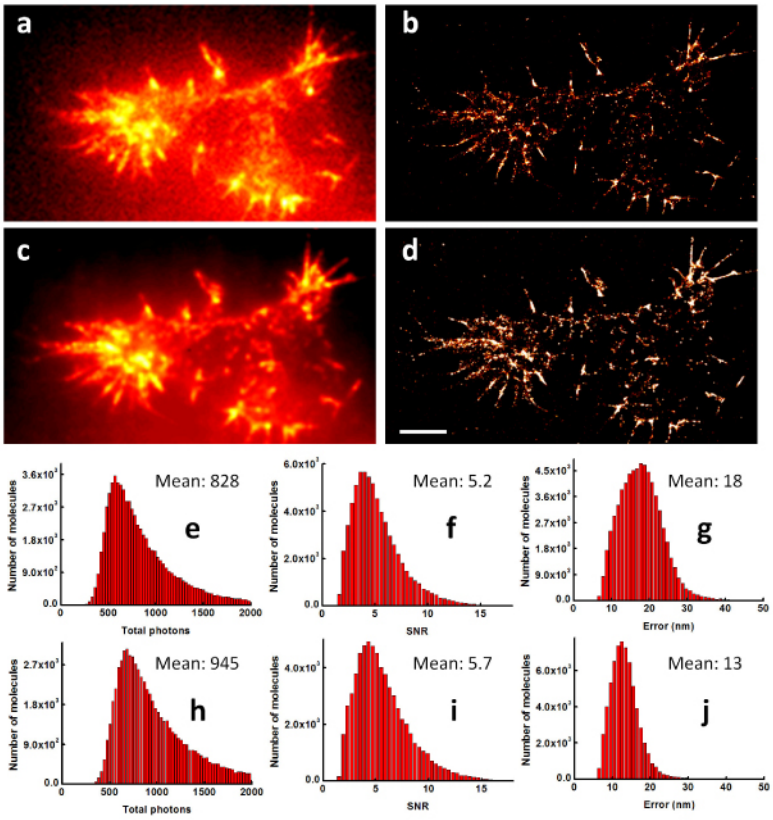

Fig. 3. Comparison of the performance of the Flash 2.8 sCMOS camera (subset 1 in a, b, e, f and g) and the iXon 897 EMCCD camera (subset 2 in c, d, h, i and j) in TIRF microscopy (a, c) and localization microscopy (b, d) imaging of actin bundles in fixed HEK293T cells labeled with d2EosFP. A stack of 2000 image frames was firstly captured with the Flash2.8 sCMOS

#151443 - $15.00 USD Received 22 Jul 2011; revised 31 Aug 2011; accepted 5 Sep 2011; published 19 Sep 2011

(Exposure time = 30 ms; Gain = 8; Binning = 2; In 184 x 104 pixels after binning; Effective pixel size at sample = 145 nm), and then another stack of 2000 image frames was obtained with the iXon 897 EMCCD (Exposure time = 30 ms; Gain = 120; No binning; In 167 x 94 pixels; Effective pixel size at sample = 160 nm). Note that the overall photon collection efficiency in these two camera ports is found to be almost identical. Histograms of total collected photons (e, h), signal-noise-ratio (f, i), and localization precision measured in standard deviation (g, j) from single molecules (Upper row: sCMOS; Lower row: EMCCD). The mean values of individual histograms are shown in the right corner of the corresponding figures. The total number of localized molecules is 68108 in (b) and 66353 in (d), respectively. Scale bars: 3 μm.

3.2 The noise performance of sCMOS in LM

Next, we investigated the reason why sCMOS could be successfully used in single molecule imaging and localization. Generally, for a low light detector used in single molecule imaging, it is of primary importance to obtain sufficient visibility for single molecules in each image frame, thus two separate issues need to be considered. The first one is signal-noise-ratio (SNR), which is defined as detected signals divided by total noise. The second one is detectability, which is determined by the smallest photon signal that can be detected from the total noise associated with this measurement. Apparently, the noise performance of a low light detector is crucial to its visibility.

Notice that the total noise of a cooled EMCCD or sCMOS camera comes mainly from signal shot noise, read noise and fixed pattern noise. And, it is clear that the main advantage of EMCCD over other detectors is from its electron multiplying mechanism, which effectively eliminates read noise [1]. However, with the advent of brighter fluorescence probes for LM [15], signal shot noise may become more significant that read noise. To verify this assumption, it is necessary to determine precisely the contribution of different noise sources to the total noise.

In fact, a well-accepted technique called photon transfer curve (PTC) measurements [13] is well-suited for characterizing the noise performance of CCD or CMOS camera. Therefore, we built an optical setup for measuring the PTC of the two cameras used in this study (Fig. 2). Representative PTC measurement results are shown in Fig. 4 and Fig. 5, where the fixed pattern noise was found to be almost negligible unless the signal is close to the detector's saturation. The spatial read noise of the Flash 2.8 sCMOS was found to be 3.7 e- for Gain = 8 and Bin = 1, 7.0 e- for Gain = 8 and Bin = 2, and 9.3 e- for Gain = 1 and Bin = 2, respectively. Interestingly, both the spatial and temporal read noise (Fig. 6) reach minimum when the on-chip analogy gain (Gain) is set to 8 and there is no binning in the Flash2.8 sCMOS. For the Andor 897 EMCCD, the spatial and temporal read noise are the same and could be effectively reduced from ~51 e- to less than 0.5 e- when electron-multiplying gain (M) is set to be larger than 120.

Furthermore, it was found that the excess noise in EMCCD [18] adds a significant contribution to the total noise (Fig. 5, middle and bottom curves), which effectively reduces the photon sensitivity of EMCCD. Figure 5 also shows that the contribution of the fixed pattern noise to the total noise is not negligible in EMCCD (especially when the signal level is high), which decreases the usefulness of EMCCD in the localization of single molecules with bright fluorescence. Unfortunately, the fixed pattern noise in sCMOS (Fig. 4) is also a troublesome issue and should be paid attention in designing LM experiments.

#151443 - $15.00 USD Received 22 Jul 2011; revised 31 Aug 2011; accepted 5 Sep 2011; published 19 Sep 2011

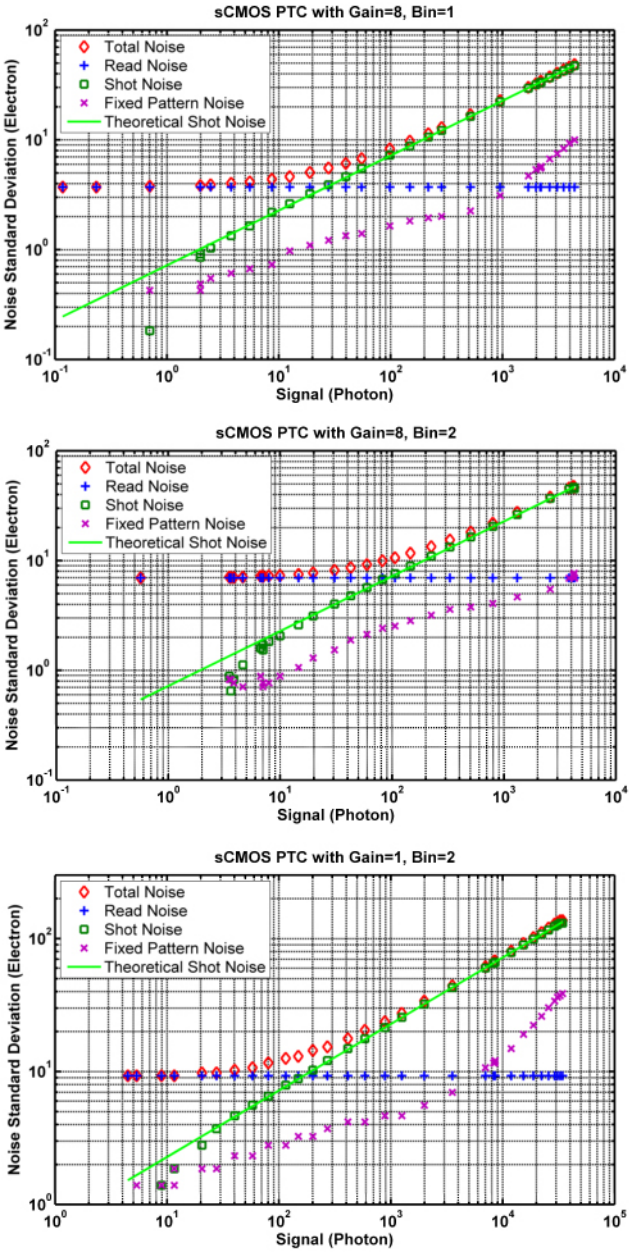

Fig. 4. Representative PTCs for the Flash2.8 sCMOS. Note that: (a) For the PTC with Gain = 8 and Bin = 1 (top curve), the image frames (signal > 2200 photons) close to detector's saturation are obtained by increasing exposure time from 50 ms to 100 ms because of the insufficient illumination intensity. (b) For the PTC with Gain = 1 and Bin = 2 (bottom curve), the image frames (signal > 11000 photons) close to detector's saturation are obtained by increasing exposure time from 50 ms to 200 ms because of the insufficient illumination intensity. (c) These are representative curves selected from three repeated measurements, which gave almost identical results. (d) The PTC for Gain = 1 and Bin = 1 was not measured, because a much stronger illumination intensity necessary for this measurement could not be obtained from our tungsten-halogen light source. (e) The camera conversion factor, K_{ADC}(e/DN), is 0.609 e/DN for Gain = 8 & Bin = 1, 0.590 e/DN for Gain = 8 & Bin = 2, and 4.65 e/DN for Gain = 1 & Bin = 2, respectively. (f) Theoretical Shot Noise is calculated by the square root of Signal*QE [13], where the QE is the quantum efficiency (photon sensitivity) of the Flash2.8 sCMOS in 580 nm and is set to be 0.52.

#151443 - $15.00 USD Received 22 Jul 2011; revised 31 Aug 2011; accepted 5 Sep 2011; published 19 Sep 2011

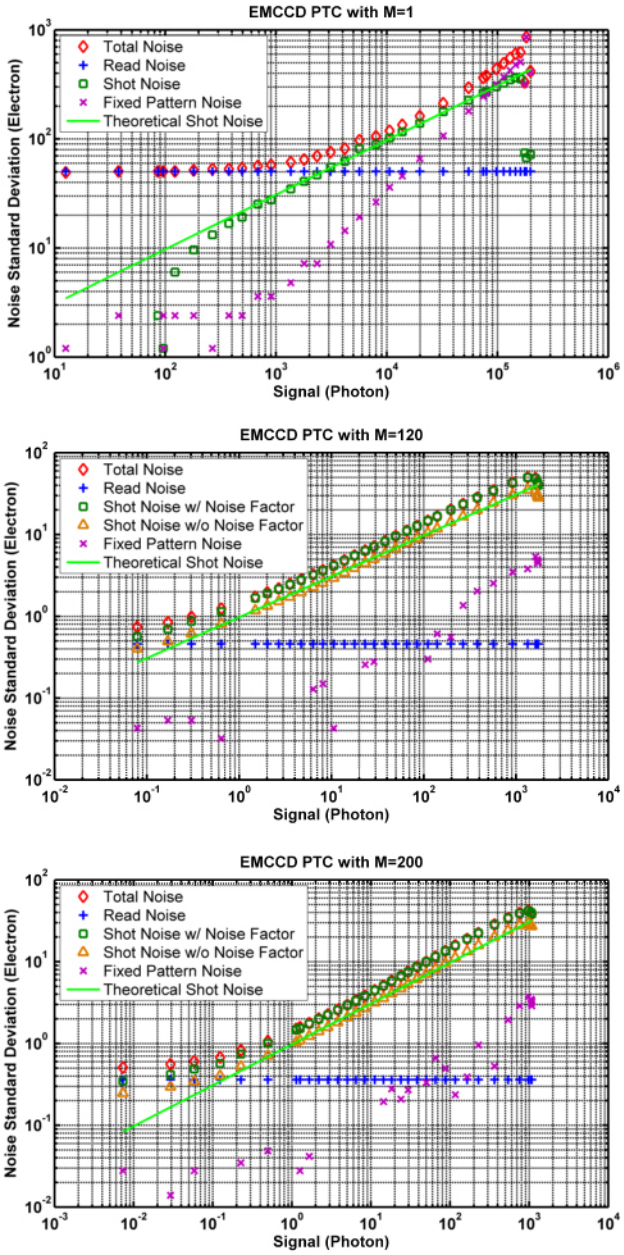

Fig. 5. Representative PTCs for the iXon 897 EMCCD. Note that (a) For the PTCs with EM Gain = 1 (top curve), the image frames (signal > 100000 photons) close to detector's saturation are obtained by increasing exposure time from 50 ms to 120ms because of the insufficient illumination intensity. (b) These are representative curves selected from three repeated measurements, which gave almost identical results. (c) The camera conversion factor, K_{ADC}(e/DN), is 12.0 e/DN for M = 1, 0.107 e/DN for M = 120, and 0.0695 e/DN for M = 200, respectively. (d) The shot noise without noise factor (Shot Noise w/o Noise Factor) is from the Shot Noise w/ Noise Factor (that is, the shot noise in Section 2.4, Eq. (5) divided by the excess noise factor, which is 1 for M = 1, and $\sqrt{2}$ for M > 100, respectively [18]. (e) Theoretical Shot Noise was calculated by the square root of Signal*QE [13], where the QE is the quantum efficiency (photon sensitivity) of the iXon 897 EMCCD in 580 nm and is set to be 0.95.

#151443 - $15.00 USD Received 22 Jul 2011; revised 31 Aug 2011; accepted 5 Sep 2011; published 19 Sep 2011

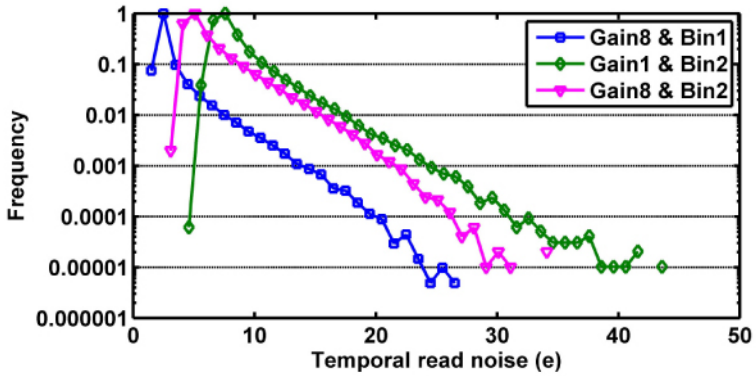

Fig. 6. The temporal read noise distribution of the Flash2.8 sCMOS. Note that the temporal read noise is reported to be 3.0 e- (rms) for Gain = 8 & Bin = 1 by the Vendor.

3.3 The detectability of sCMOS in LM

With the PTC measurement results, we calculated that the detectability of the Flash2.8 sCMOS is 29 photons in the best case (Table 1, Gain = 8, Bin = 1). After a further analysis on the contributions from different noise sources to the total noise in Fig. 3a, we found out that the shot noise is 12.5 e- from fluorescence background and 8.8 e- from signal, respectively (Table 1). While for the same image, the read noise from the sCMOS is as small as 3.0 e-. Clearly, with a bright fluorescence probe such as d2EosFP, LM imaging is now working in the shot noise limited region (See the arrows in Fig. 7), where efforts on minimizing background photon (that is, increasing SBR) is of particularly important for obtaining good LM results (Table 1).

In a previous report [11], we found out that EMCCD shows notable advantages than sCMOS in single molecule localization only when the total number of detected photons is less than 300 and the signal-background-ratio (SBR) is high (>2). However, in practical LM experiments (especially for those without TIRF illumination), the total number of detected photons would be larger than 1000 photons [10] and the signal would be usually embedded in a strong fluorescence background (SBR < 1) [19]. In this case, sCMOS is suitable to be used as a replacement detector for EMCCD.

#151443 - $15.00 USD Received 22 Jul 2011; revised 31 Aug 2011; accepted 5 Sep 2011; published 19 Sep 2011

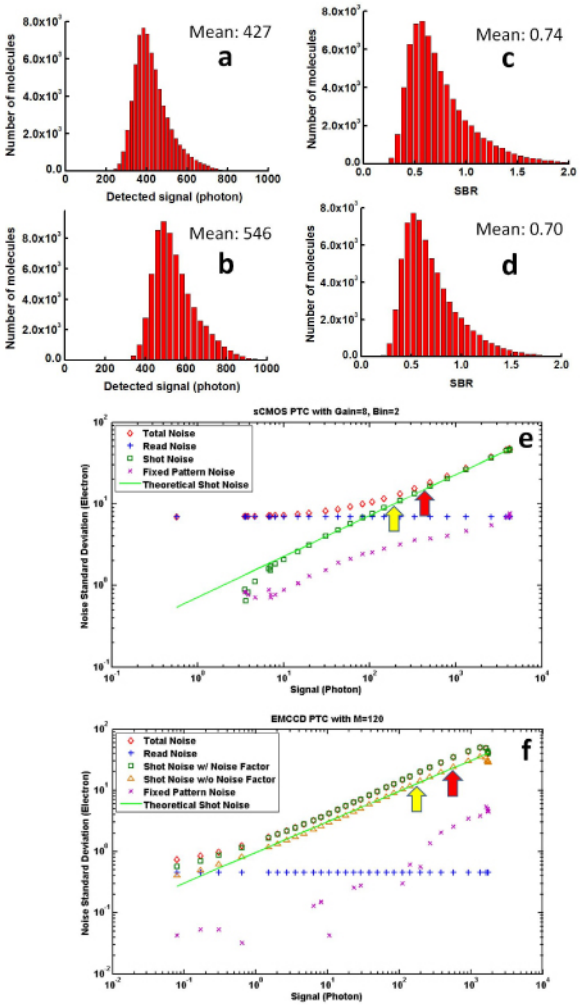

Fig. 7. Comparison on the visibility of single molecule embedded in background noise by the Flash2.8 sCMOS (subset 1 in a, c and e) and the iXon 897 EMCCD (subset 2 in b, d and f). Histograms of the detected emission in the peak pixel after dark image offset subtraction (a, b), signal-background-ratio (c, d) from single molecules (Upper row: sCMOS; Lower row: EMCCD). Note that the histograms are obtained from analyzing Fig. 3b and Fig. 3d. The mean values of individual histograms are shown in the right corner of the corresponding figures. The photon transfer curves of the Flash2.8 sCMOS (e) and the iXon 897 EMCCD (f) were measured with the same camera settings as those in Fig. 3. The red arrows in (e) and (f) indicate the corresponding mean values of (a) and (b), which are originated from a combination of signal fluorescence and background fluorescence. The yellow arrows in (e) and (f) indicate the detected mean values of signal fluorescence, which was calculated from detected signal and SBR. The difference between the theoretical shot noise and total noise in (f) indicates the contribution of excess noise in EMCCD.

Table 1. Detectability of the Flash2.8 sCMOS and the iXon 897 EMCCD

	EMCCD (M = 120)	sCMOS Gain=8, Bin=2	Gain=8, Bin=1
σ_{Read} (e-) [a]	0.4	6.3	3.0
Detectability [b] (photon)	2	61	29
$\sigma_{shot,bkg}$ [c] (e-)	17.5	11.3	12.5
$\sigma_{shot,signal}$ [d] (e-)	14.6	9.7	8.8

(a) Read noise. Note that the dark charge noise is 1 e/pix/s @ 20 °C in the Flash2.8 sCMOS and 0.001 e/pix/s @ –60 °C in the iXon 897 EMCCD, respectively. (b) The detectability is defined as the smallest photon signal (S_{ph}) whose

#151443 - $15.00 USD Received 22 Jul 2011; revised 31 Aug 2011; accepted 5 Sep 2011; published 19 Sep 2011

magnitude equals to that of total noise. The photon shot noise (equals to the square root of S_{ph}) is negligible when S_{ph} is small, then the total noise is equal to read noise. Considering that peak-to-peak noise is ~5 times the rms value [20], the detectabity can be calculated by (σ_{Read}*5)/QE. (c) Shot noise from fluorescence background, which is calculated from the detected emission in the peak pixel after dark image offset subtraction (Fig. 3). Both signal photons and background fluorescence contribute to the detected emission. (d) Shot noise from single molecule.

4. Conclusion

We verified experimentally the applicability of a Hamamatsu ORCA-Flash2.8 sCMOS in localization microscopy. We characterized the contribution of different noise sources to the total noise of the sCMOS in single molecule imaging, and found out that localization microscopy is now working in the shot noise limited region with the use of a bright fluorescence probe such as d2EosFP. With the advent of brighter fluorescence probes, replacing EMCCD with sCMOS is possible and would be even advantages for exploring the versatility and power of localization microscopy in broader biological applications.

Acknowledgements

This work was supported by National Basic Research Program of China (Grant No. 2011CB910401), the National Natural Science Foundation of China (Grant Nos. 30970691 and 30925013), the Program for New Century Excellent Talents in University of China (Grant No. NCET-10-0407 to Z.L.H.), the Fundamental Research Funds for the Central Universities (Grant Nos. 2010ZD028 and 2011TS087). We thank Prof. Gerd Ulrich Nienhaus and Mr. Per Niklas Hedde from Karlsruhe Institute of Technology for the d2EosFP plasmid and helpful discussions, Prof. Bo Huang from University of California-San Francisco for helpful discussions and suggestions. We appreciate Mr. Tadashi Maruno, Mr. Eiji Toda and Dr. Keith Bennett from Hamamatsu for the loan and technical support on the ORCA-Flash2.8 sCMOS and helpful discussions. We also thank the technical support from the Analytical and Testing Center of Huazhong University of Science and Technology.

#151443 - $15.00 USD Received 22 Jul 2011; revised 31 Aug 2011; accepted 5 Sep 2011; published 19 Sep 2011